Hindawi Publishing Corporation
Mathematical Problems in Engineering
Volume 2015, Article ID 854085, 10 pages
http://dx.doi.org/10.1155/2015/854085

Research Article

Adaptive Fusion Design Using Multiscale Unscented Kalman Filter Approach for Multisensor Data Fusion

Huadong Wang[1] and Shi Dong[1,2]

[1]*School of Computer Science and Technology, Zhoukou Normal University, Zhoukou 466001, China*
[2]*School of Computer Science and Technology, Huazhong University of Science and Technology, Wuhan 430074, China*

Correspondence should be addressed to Shi Dong; njbsok@gmail.com

Received 28 July 2015; Revised 26 October 2015; Accepted 27 October 2015

Academic Editor: Fernando Torres

In order to improve the reliability of measurement data, the multisensor data fusion technology has progressed greatly in improving the accuracy of measurement data. This paper utilizes the real-time, recursive, and optimal estimation characteristics of unscented Kalman filter (UKF), as well as the unique advantages of multiscale wavelet transform decomposition in data analysis to effectively integrate observational data from multiple sensors. A new multiscale UKF-based multisensor data fusion algorithm is proposed by combining the UKF with multiscale signal analysis. Firstly, model-based UKF is introduced into the multiple sensors, and then the model is decomposed at multiple scales onto the coarse scale with wavelets. Next, signals decomposed from fine to coarse scales are adjusted using the denoised observational data from corresponding sensors and reconstructed with wavelets to obtain the fused signals. Finally, the processed data are fused using adaptive weighted fusion algorithm. Comparison of simulation and experimental results shows that the proposed method can effectively improve the antijamming capability of the measurement system and ensure the reliability and accuracy of sensor measurement system compared to the use of data fusion algorithm alone.

1. Introduction

Multisensor data fusion is one of the key technologies for achieving intelligent measurement. Data measured with a single sensor are often incomplete, have great uncertainty, or even contain abnormal noise point due to the accuracy, resolution, measurement noise, and other factors of single sensor [1]. Meanwhile, susceptible to factors like measurement noise, sensor type, number of nodes, and monitoring location and influenced by formal uncertainties, diversity, quantitative enormousness, relational complexity, and redundancy of information detected, the sensor detection data are prone to be unreliable, incomplete, inaccurate, ambiguous, or even contradictory. Multisensor data fusion is a commonly used method of improving measurement accuracy and reliability. Multisensor data fusion technology has been widely used in military application domains such as automatic target recognition, battlefield surveillance, and traffic control, as well as nonmilitary application areas such as complex machine system monitoring, robotics, and medical diagnostics. Existing data fusion methods are divided into classic fusion methods and modern intelligent fusion algorithms [2, 3]. Weighted average method, least squares method, likelihood estimation, Kalman filtering, group-Bayes estimation, and D-S evidence reasoning are the representatives of classic fusion algorithms, whereas major modern intelligent fusion algorithms include expert system, cluster analysis, production rule, rough set theory, and neural network [4, 5]. The problem of data fusion for multisensor has been addressed by several exiting works in the context of data processing. In traditional simple multisensory data fusion algorithms, measurement accuracy is poor and there is low fusion efficiency, resulting in measurement uncertainty. How to design a high accuracy of the new algorithm has been the integration of multisensor data fusion research priorities. Zhao and Wang [6] proposed extended Kalman filter (EKF)

for multisensors data fusion; experimental results show that the accumulated errors of inertial sensors are reduced by ultrasonic sensors and magnetometers, and EKF improves the accuracy of orientation and position measurements. Chiou and Tsai [7] presented a low-complexity and high-accuracy algorithm to reduce the computational load of the traditional data fusion algorithm with heterogeneous observations for location tracking. Not only can the proposed approach achieve an accurate location close to that of the traditional Kalman filtering data fusion algorithm but also it has much lower computational complexity. Ligorio and Sabatini [8] used a linear Kalman filter where the sensor fusion between triaxial gyroscope and triaxial accelerometer data was performed. A significant accuracy improvement was achieved over state-of-the-art approaches, due to a filter design that better matched the basic optimality assumptions of Kalman filtering. Vaccarella et al. [9] proposed a sensor fusion algorithm to compensate for the drawbacks of optical tracking systems (OTS) and electromagnetic tracking systems (EMTS) and achieve robust tracking of surgical instruments. The proposed algorithm increases the accuracy of EMTS in the presence of magnetic field distortion. Zhang et al. [10] takes the upper limb as our research subject and present a novel upper limb movement estimation algorithm to cope with these two challenges by adaptive fusion of sensor data and human skeleton constraint. Zheng et al. [11] proposed a new framework for sequential Bayesian estimation in sensor networks; the proposed scheme outperforms the one that ignores missing data information and the one that selects sensors randomly for information transmission. Mosallaei and Salahshoor investigate the application of centralized multisensor data fusion (CMSDF) technique to enhance the process fault detection. The measurement fusion methods directly fuse observations or sensor measurements to obtain a weighted or combined measurement and then use a single Kalman filter to obtain the final state estimate based upon the fused measurement [12]. These authors presented a Particle Filter (PF) based multisensor data fusion (MSDF) technique in an integrated Navigation and Guidance System (NGS) design based on low-cost avionics sensors [13]. Wang et al. addressed the problem of tracking multiple targets using multisensor bearings-only measurements in the presence of noise and clutter. The Rao-Blackwellized Monte Carlo Data Association (RBMCDA) scheme and the unscented Kalman filter (UKF) were applied to solve the problems of uncertain association and nonlinear filtering [14]. Wang et al. proposed a multisensor data fusion technique for the online volume concentration measurement of coal/biomass pulverized-fuel flow in cofired power plant. The techniques combine electrostatic sensors with capacitance sensors and incorporate a data fusion technique based on an adaptive wavelet neural network (AWNN), and gradient descent learning algorithm and genetic learning algorithm are used for training of the network parameters [15].

At present, the wavelet transformation, combining with Kalman filter, is the most used algorithm in multisensor data fusion technology. However, wavelet transformation and Kalman filter have two aspect problems in algorithm. One aspect of the problem consists in the multiresolution analysis (MRA) method of wavelet transformation. It only subdivides the approximate signal of low-frequency band step by step effectively, which causes the precision in low-frequency band to be more and more high and that the detail signal of the high-frequency band is invariable. Therefore, MRA method has low resolving ability in frequency. The other aspect of the problem is that some system has nonlinear character in practice measuring, which makes Kalman filter precarious and even causes no convergence. So the filter effect is not very good.

In order to overcome the shortcoming described above, a new multiscale UKF-based multisensor data fusion algorithm is proposed by combining the UKF with multiscale signal analysis. The improved data fusion way is used to fuse multiresolution data in the sensor measurement system, which can fuse multisensors data in different resolution.

The main contributions of this paper are summarized as follows:

(1) A new multiscale UKF-based multisensor data fusion algorithm is proposed by combining the UKF with multiscale signal analysis.

(2) We provide extensive numerical results to demonstrate the usage and efficiency of the proposed multisensor data fusion algorithm.

(3) We evaluate the performance of the proposed algorithms by comparing them with the use of data fusion algorithm alone. The proposed method can effectively improve the antijamming capability of the measurement system and ensure the reliability and accuracy of sensor measurement system.

2. System Description

By the dynamic equation and observation equation of the Kalman filtering algorithm, which can get m sensor signal at a scale of i ($1 \leqslant i \leqslant S$) system model,

$$x(i,k+1) = A(i,k)\,x(i,k) + v(i,k), \quad (k \geqslant 0), \tag{1}$$

wherein, in formula (1), $x(i,k)$ is n-dimensional matrix, $x(i,k) \in R^{n\times 1}$, $A(i,k)$ is a system matrix, $A(i,k) \in R^{n\times n}$, and $v(i,k)$ is the systematic noise, $v(i,k) \in R^{n\times 1}$, and satisfies the following statistical properties:

$$\begin{aligned} E\{v(i,k)\} &= 0, \\ E\left\{v(i,k)\,v^T(i,k)\right\} &= Q(i,k)\,\delta_{kl}. \end{aligned} \tag{2}$$

The general observation equation is

$$Z(i,k) = C(i,k)\,x(i,k) + w(i,k), \quad k \geq 0, \tag{3}$$

wherein

$$Z(i,k) = \begin{bmatrix} z_1(i,k) \\ z_2(i,k) \\ \vdots \\ z_m(i,k) \end{bmatrix},$$

$$C(i,k) = \begin{bmatrix} c_1(i,k) \\ c_2(i,k) \\ \vdots \\ c_m(i,k) \end{bmatrix}, \quad (4)$$

$$w(i,k) = \begin{bmatrix} w_1(i,k) \\ w_2(i,k) \\ \vdots \\ w_m(i,k) \end{bmatrix},$$

where, in formula (3), the observed value $Z_j(i,k) \in R^{P_j \times 1}$ represents the observed values of the jth sensor on the scale i ($1 \leqslant i \leqslant S$), $j = 1, 2, \ldots, m$, the sampling rate of the sample between the two dimensions of the sensor vector is 2:1, namely, $x(i,k) = x(N, 2^{N-i}k)$, $C_j(i,k) \in R^{P_j \times n}$ is observation matrix, and observation noise $w_j(i,k) \in R^{P_j \times 1}$ is Gauss white noise sequence. At the same time,

$$E\{w(i,k)\} = 0$$
$$E\left\{w(i,k)\, w^T(i,k)\right\} = R(i,k)\, \delta_{kj}. \quad (5)$$

Here we assumed that $x(N,k)$, $w(N,k)$, and $v(i,k)$ are uncorrelated.

3. Unscented Kalman Filter and Wavelet Transform

3.1. Unscented Kalman Filter. Unscented Kalman filter (UKF) is a Gaussian filter which calculates the mean and covariance of nonlinear transformation using unscented transform (UT). Based on the principle that the approximate probability distribution is easier than the approximate arbitrary nonlinear transformation, the UT (1) characterizes certain characteristics, such as mean and covariance, of a probability distribution by deterministically selecting a set of sample points; (2) propagates this set of sample points through the nonlinear transformation; and (3) calculates the mean and covariance of propagated sample points. Estimation accuracy of UKF depends on the accuracy of mean and covariance calculated by UT. Compared to the extended Kalman filter (EKF), UKF offers better performance at the same amount of calculation and does not require the calculation of Jacobian matrix. It can be interpreted as random linear regression, thereby revealing the reason why UKF is superior to EKF. Existing UKF algorithm is essentially a second-order UT-based nonlinear filtering method, which can only match the second-order Taylor expansion terms of nonlinear function, and therefore has a limited accuracy.

Implementation steps of the unscented Kalman filter are as follows:

(1) Calculating weights w_i corresponding to sample points using $\widehat{x}_{k-1|k-1}$ and $P_{k-1|k-1}$ given previously, $w_i^m = w_i^c = 0.5/(L+\lambda)$, here $i = 1, 2, \ldots, 2L$, λ is the dispersion degree of sample points, w_i^m is the weight coefficient of the first-order statistical properties, and w_i^c is a function of second-order statistical properties of the required weight coefficients.

(2) Propagation function of the state evolution equation related to the sample points should be calculated as follows: $x_i(k+1 \mid k) = f(x_i(k \mid k))$.

(3) The statistical characteristic functions $\widetilde{x}(k+1 \mid k)$ and $P(k+1 \mid k)$ should be calculated assisted with forecast sampling points $x_i(k+1 \mid k)$ and weights w_i,

$$\widetilde{x}(k+1 \mid k) = \sum_{i=0}^{2L} w_i^m x_i(k+1 \mid k),$$
$$P(k+1 \mid k) = Q(K+1) + \sum_{i=0}^{2L} w_i^c \left[x_i(k+1 \mid k) - \widetilde{x}(k+1 \mid k)\right] \cdot \left[x_i(k+1 \mid k) - \widetilde{x}(k+1 \mid k)\right]^T. \quad (6)$$

(4) Calculation of dispersion function derived from measurement equation of sample points that are obtained by utilizing UT transformation, $y_i(k+1 \mid k) = hx_i(k+1 \mid k)$.

(5) The predicted value and the measured value of the statistical characteristics should be calculated by $\widetilde{z}(k+1 \mid k) = \sum_{i=0}^{2L} w_i^m y_i(k+1 \mid k)$,

$$P_{ZZ} = R(K+1) + \sum_{i=0}^{2L} w_i^c \left[y_i(k+1 \mid k) - \widetilde{z}(k+1 \mid k)\right] \cdot \left[y_i(k+1 \mid k) - \widetilde{z}(k+1 \mid k)\right]^T,$$
$$P_{XZ} = \sum_{i=0}^{2L} w_i^c \left[x_i(k+1 \mid k) - X(k+1 \mid k)\right] \cdot \left[y_i(k+1 \mid k) - \widetilde{z}(k+1 \mid k)\right]^T. \quad (7)$$

Here P_{ZZ} is the measurement error covariance matrix, P_{XZ} is the covariance matrix of the state vector and the measured values.

(6) Amplification of unscented Kalman filter should be calculated; simultaneously, it is required to update system characteristic function $K(k+1) = P_{XZ} \cdot {P^{-1}}_{ZZ}$,

$$\begin{aligned}&\widetilde{x}(k+1 \mid k+1)\\&\quad = \widetilde{x}(k+1 \mid k)\\&\qquad + K(k+1)\left(z(k+1) - \widetilde{z}(k+1 \mid k)\right),\end{aligned} \tag{8}$$

$$\begin{aligned}&P(k+1 \mid k+1)\\&\quad = P(k+1 \mid k) - K(k+1) P_{ZZ} K^{T}(k+1).\end{aligned} \tag{9}$$

It can be seen from the implementation process of UKF that its estimation of mean and variance is actually accurate to the Taylor expanded quadratic polynomial of function $h(x)$, while EKF can only be accurate to linear item generally, and other higher-order nonlinear polynomials are all ignorable. Therefore, UKF is easy to implement, has higher estimation accuracy than EKF, and can be applied to any linear model.

Although UKF has been widely used in the estimation of dynamic systems, it is established based on the dynamic model and observation model of target in the time domain, which does not take into account the multiscale characteristics of target and is unable to conduct multiscale analysis on target data. Wavelet transform, as a powerful multiscale analytical tool, just makes up for the deficiency of UKF in multisensor multiscale analysis.

3.2. Wavelet Transform. In recent years, wavelet analysis has become a rapidly developing emerging discipline. Wavelet transform offers a multiresolution, microscopic way of image representation that is suited to the human vision principle [16]. After many years of development, a series of remarkable theoretical and practical achievements have been made on wavelet transform, which has been widely used in the scientific and technological fields such as signal processing, image processing, speech recognition and synthesis, radar, CT imaging, pattern recognition, machine vision, and machine fault diagnosis [17, 18]. Wavelet transform makes localized temporal (spatial) frequency analysis on signals gradually refine function in a multiscale manner through stretching and translation operations and thereby ultimately achieve temporal subdivision of signals at high frequencies and frequency subdivision of signals at low frequencies, which can automatically adapt to the requirements of time-frequency signal analysis [19, 20]. In this paper, multiscale stochastic dynamic models at different scales are built using combined multiscale signal representation and data fusion technologies based on a dynamic system with different characteristics at different scales where multiple sensors are used to observe the same random phenomenon (target state) to obtain some effective state estimation and reconstruction algorithms.

Define $\psi(t) \in L^2(R)$, when it meets the allowable conditions,

$$C\psi = \int_{-\infty}^{+\infty} \frac{\left|\widehat{\psi}(w)\right|^2}{|w|} dw < \infty, \tag{10}$$

wherein $\psi(w)$ is $\psi(t)$ Fourier transform; then call $\psi(t)$ based wavelet. The wavelet function generated by $\psi(t)$ can be expressed as

$$\psi_{a,b}(t) = |a|^{-1/2} \psi\left(\frac{t-b}{a}\right), \tag{11}$$

where b is the translation factor and a is the scale factor.

Define $f(t) \in L^2(R)$; then the based wavelet function $\psi_{a,b}(t)$ continuous wavelet transform is as follows:

$$\left(W\psi f\right)(a,b) = \int_{-\infty}^{+\infty} f(t) \overline{\psi_{a,b}(t)} dt. \tag{12}$$

After expanding a, b, frequency spectrum of any time with any precision can be obtained. For actual operation, its data size is too big, so parameters a, b are discretized to obtain discrete wavelet transform. Its corresponding discrete wavelet function can be expressed as

$$\psi_{j,k}(t) = {a_0}^{-j/2} \psi\left({a_0}^{-j} t - k b_0\right), \quad j,k \in Z. \tag{13}$$

Discrete wavelet transform coefficients can be expressed as

$$W_{j,k}(t) = \int_{-\infty}^{+\infty} f(t) \overline{\psi_{j,k}(t)} dt. \tag{14}$$

The reconstruction formula is

$$f(t) = C \sum_{-\infty}^{\infty} \sum_{-\infty}^{\infty} W_{j,k} \psi_{j,k}(t). \tag{15}$$

If the discrete point is $a0 = 2$, $b0 = 1$, which is called the binary wavelet transform.

Considering signal sequence $x(i+1,k) \in (l^2)^n$, $(k \in Z)$ with scale $i+1$, the analysis and integrated form of discrete orthogonal wavelet transform are $x(i,k) = \sum_l h(2k-l)x(i+1,l)$, $d(i,k) = \sum_l g(2k-l)x(i+1,l)$, and $x(i+1,k) = \sum_l h(2k-l)x(i,l) + \sum_l g(2l-k)d(i,l)$, where $x(i,k)$ and $d(i,k)$ are, respectively, smooth signal and detail signal of $x(i+1,k)$, $h(k)$ and $g(k)$, respectively, correspond to the low-pass filter and high-pass filter. In the wavelet transform, the processing procedure is as follows: firstly, original signal is decomposed into the low-frequency approximate section and the high-frequency detail section; what follows are all further decompositions of low-frequency approximate section of signal, while high-frequency detail section is not considered.

4. Multiscale Representation Method of Signal

Assuming that the signal sequence $\{x(i,k)\}_{k \in Z}$ is divided into data blocks with length $M_i = 2^{i-1}$ $(i = N, \ldots, L, M, M_N)$,

$$\begin{aligned}X_m(i) = \Big|&x^T\left(i, mM_i + 1\right), x^T\left(i, mM_i + 2\right), \ldots,\\&x^T\left(i, mM_i + M_i\right)\Big|^T.\end{aligned} \tag{16}$$

The dynamic relationship between status variable data block $X_{m+1}(N)$ and $X_m(N)$ can be described as

$$\begin{aligned}
&X_{m+1}(N) = A_m(N) X_m(N) + W_m(N),\\
&A_m(N) = \operatorname{diag}\left\{\prod_{K=M}^{1} A(N, mM+k), \prod_{K=M+1}^{1} A(N, mM+k), \ldots, \prod_{K=2M-1}^{1} A(N, mM+k)\right\},\\
&W_m(N) = B_m(N)\begin{bmatrix} w(N, mM+1)\\ \vdots\\ w(N, mM+M)\\ \vdots\\ w(N, mM+2M-1)\end{bmatrix},\\
&B_m(N) = \begin{bmatrix} \prod_{K=M}^{2} A(N, mM+k) & \prod_{K=M}^{3} A(N, mM+k) & \cdots & 1 & \cdots & 0\\ 0 & \prod_{K=M+1}^{3} A(N, mM+k) & \cdots & A(N, mM+M+1) & \cdots & 0\\ \vdots & \vdots & \ddots & \vdots & \cdots & \vdots\\ 0 & 0 & 0 & \prod_{K=2M-1}^{M+1} A(N, mM+k) & \cdots & 1\end{bmatrix}.
\end{aligned} \tag{17}$$

$Wm(N)$ has statistical properties $E\{W_m(N)\} = 0$,

$$\begin{aligned}
&E\left\{W_m(N) {W_m}^T(N)\right\} = B_m(N) Q_m(N) {B_m}^T(N),\\
&Q_m(N) = \{Q(N, mM+1), Q(N, mM+2), \ldots,\\
&\quad Q(N, mM+2M-1)\}.
\end{aligned} \tag{18}$$

Meanwhile, with regard to scale value i, observation value and error, symbolled as $Z_m(i)$ and $V_m(i)$, respectively, can be written in the form of data blocks as (9) shows; then we have the following equalities

$$\begin{aligned}
&Z_m(i) = C_m(i) X_m(N) + V_m(i),\\
&C_m(i) = \operatorname{diag}\{C(i, mM_i+1)\delta(i), \ldots, C(i, mM_i+M_i)\\
&\quad \cdot \delta(i)\}.
\end{aligned} \tag{19}$$

$\delta(i)$ is a matrix of $n \times n^{2N-I}$ dimension, where the ultimate n columns compose a single matrix and other elements are zero. $V_m(i)$ has statistical properties $E\{Vm(i)\} = 0$,

$$\begin{aligned}
&R_m(i) = \operatorname{diag}\{R(i, mM_i+1), R(i, mM_i+2), \ldots,\\
&\quad R(i, mM_i+M_i)\},\\
&E\left\{V_m(i) {V_m}^T(i)\right\} = R_m(i).
\end{aligned} \tag{20}$$

5. Multiscale Information Fusion Estimation Algorithm

The initial values of data block $X_m(N)$ are $X_{0|0}(N)$ and $P_{0|0}(N)$; they can be calculated by the following equation:

$$\begin{aligned}
&X_{0|0}(N) = \begin{bmatrix} X(N,1)\\ X(N,2)\\ \vdots\\ X(N,M)\end{bmatrix} = \overline{A}_0(N) x_0,\\
&P_{0|0}(N) = \overline{A}_0(N) P_0 {\overline{A}_0}^T(N) + \overline{B}_0(N) Q_0 {\overline{B}_0}^T(N),\\
&\overline{A}_0(N) = \begin{bmatrix} A(N,0)\\ A(N,1)A(N,0)\\ \vdots\\ \prod_{k=M-1}^{0} A(N,k)\end{bmatrix},\\
&\overline{B}_0(N) = \begin{bmatrix} 1 & 0 & \cdots & 0\\ A(N,0) & 1 & \cdots & 0\\ \vdots & \vdots & \ddots & \vdots\\ \prod_{k=M-2}^{0} A(N,k) & \prod_{k=M-2}^{1} A(N,k) & \cdots & 1\end{bmatrix},
\end{aligned}$$

$$\overline{Q}_0(N) = \operatorname{diag}\{Q(N,0), Q(N,1), \ldots, Q(N,M-1)\}. \quad (21)$$

Assuming that estimation value $X_{m|m}(N)$ of the mth state vector $X_m(N)$ and estimation covariance error matrix $P_{m|m}(N)$ corresponding to $X_{m|m}(N)$ have been obtained, both of them are based on global information fusion; therefore, the following equations can be concluded:

$$\begin{aligned}
&X_{m+1|m+1}(N) = P_{m+1|m+1}(N) \\
&\quad \cdot \left[\sum_{i=1}^{N} P^{-1}_{i,m+1|m+1} X_{i,m+1|m+1}(N) \right. \\
&\quad \left. - (N-1) P^{-1}_{m+1|m+1}(N) X_{m+1|m+1}(N) \right], \\
&P^{-1}_{m+1|m+1}(N) = P^{-1}_{m+1|m}(N) \\
&\quad + \sum_{i=1}^{N} \left| P^{-1}_{i,m+1|m+1}(N) - P^{-1}_{i,m+1|m}(N) \right|, \\
&X_{i,m+1|m+1}(N) = X_{m+1|m+1}(N) + K_{i,m+1}(N) \\
&\quad \cdot \left[Z_{m+1}(i) - C_{m+1}(i) X_{m+1|m}(N) \right], \\
&X_{m+1|m}(N) = A_m(N) X_{m|m}(N), \\
&P_{m+1|m}(N) = A_m(N) P_{m|m}(N) A_m{}^T(N) + B_m(N) \\
&\quad \cdot Q_m(N) B_m{}^T(N), \\
&K_{i,m+1}(N) = P_{m+1|m}(N) C^T_{m+1}(i) \\
&\quad \cdot \left[C_{m+1}(i) P_{m+1|m}(N) C^T_{m+1}(i) + R_{m+1}(i) \right]^{-1}, \\
&P_{i,m+1|m+1}(N) = \left[1 - K_{i,m+1}(N) C_{m+1}(i) \right] P_{m+1|m}(N).
\end{aligned} \quad (22)$$

The following steps are for multiscale multisensor data fusion:

(1) A sensor signal with a given length of the time step L was defined. Firstly, UKF was applied to it, and filter estimation was made based on the observational data in UKF to obtain the estimation sequence $X(N)$. However, filtering effect was not obvious due to the substantial amount of noise contained in the data acquired from original sensors. The signal sequence obtained from filter estimation was defined as the initial sequence $X(N)$, and further correction and multiscale analysis were made on its estimated value on the scale axis.

(2) Multiscale wavelet decomposition was performed on the initial sequence $X(N)$ onto the coarsest scale i to obtain the low-frequency and high-frequency decomposition sequence $\{X_H(N-1), X_H(N-2), \ldots, X_H(i), X_L(i)\}$. Then, the wavelet decomposed low-frequency signals were further decomposed while ignoring the high-frequency detail section, and after reconstruction $X'_2(N)$ and $X'_3(N)$ were obtained. Afterwards, the wavelet decomposed low-frequency approximation section was further decomposed. Finally, the low-frequency signals obtained were reconstructed to obtain $X'(N)$. Multilevel decomposition and reconstruction procedures of collected sensor signals by UKF and wavelets are shown in Figure 1.

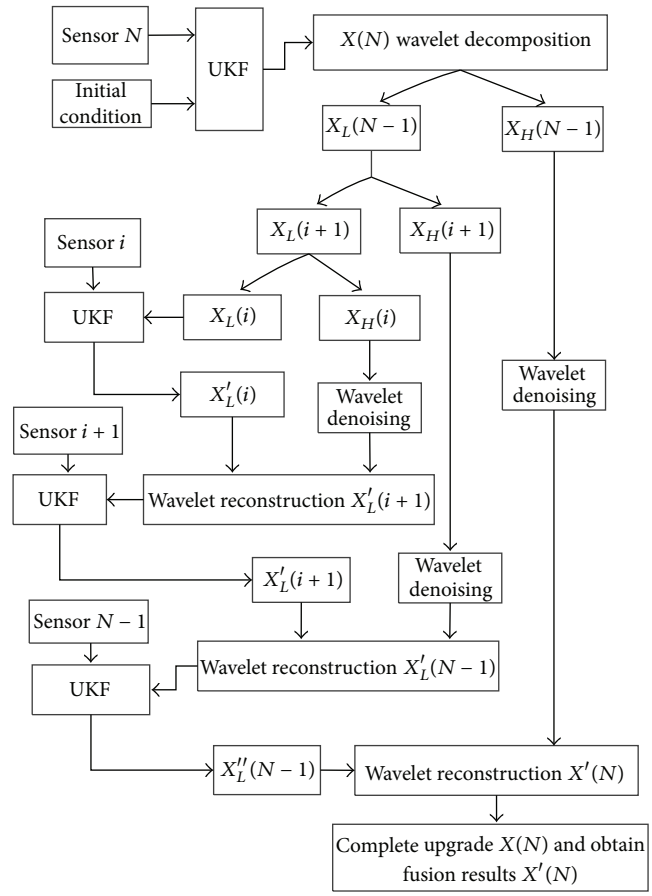

Figure 1: UKF and multiscale wavelet decomposition flowchart.

(3) Adaptive data fusion was performed on the sensor signals obtained by multiscale analysis using adaptive weighted least squares (WLS) [21], the adaptive weights $\omega_1, \omega_2, \ldots, \omega_N$. $\omega_1 + \omega_2 + \cdots + \omega_N = 1$. Achievement of weighted adaptive multisensor fusion avoids the unreliability of sensor detection data resulting from the representational uncertainty, diversity, complexity, and redundancy of detection information in the sensor networks. Multiscale multisensor adaptive weighted data fusion technology adopted in this paper avoids the uncertainty of single sensor measurement and improves the measurement accuracy and fusion efficiency. Flowchart of multiscale multisensor adaptive weighted data fusion algorithm is shown in Figure 2.

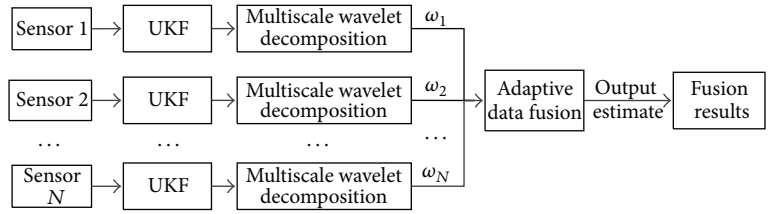

Figure 2: Multisensor data fusion algorithm diagram.

6. Performance Evolution

To examine the effectiveness of the proposed algorithm, we conducted computer simulation, as well as actual test on magnetic flux measurement of small vehicles with magnetoresistive sensors during the maneuvering target detection and recognition, which were compared for errors with the data collected by actual sensors to verify the correctness of the proposed algorithm.

(1) Analog Simulation. In the simulation test of multiscale multisensor adaptive weighted data fusion algorithm, the simulation environment was implemented in Matlab 2014a, and PC hardware parameters were Core i5 processor, 3.3 Ghz, and 8 G memory. We simulated the sinusoidal signals $X(n)$ collected by three sensors via computer, which were added with random disturbance noise to constitute the measurement signals. Measurement signals of three sensors were obtained to be $S_1 = X(n) + \text{rand}\, n(1, 1024) * 0.2$, $S_2 = X(n) + \text{rand}\, n(1, 1024) * 0.25$, and $S_3 = X(n) + \text{rand}\, n(1, 1024) * 0.3$, respectively. UKF filtering, multiscale wavelet decomposition, and adaptive data fusion were performed on these three sets of data, where we adopted db4 wavelet transform and conducted two-layer wavelet decomposition. The simulation results are shown in Figure 3. Measurement signal S_1 was taken as an example to be compared with the original signals, only using UKF.

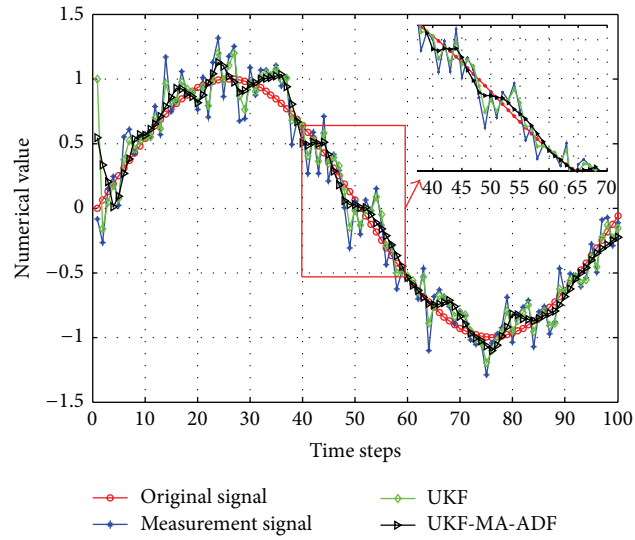

Figure 3: Simulation results of sinusoidal signal filtering processing.

As can be seen from Figure 3, UKF, multiscale wavelet analysis, and adaptive fusion algorithm are effective in filtering the measurement signals. A combination of the three algorithms allows better effects, better retention of original signals, and more stable and smooth signals. To further analyze the differences between signal processing algorithms, Figure 4 gives the comparison of errors between various algorithms by taking measurement data S_1 as an example.

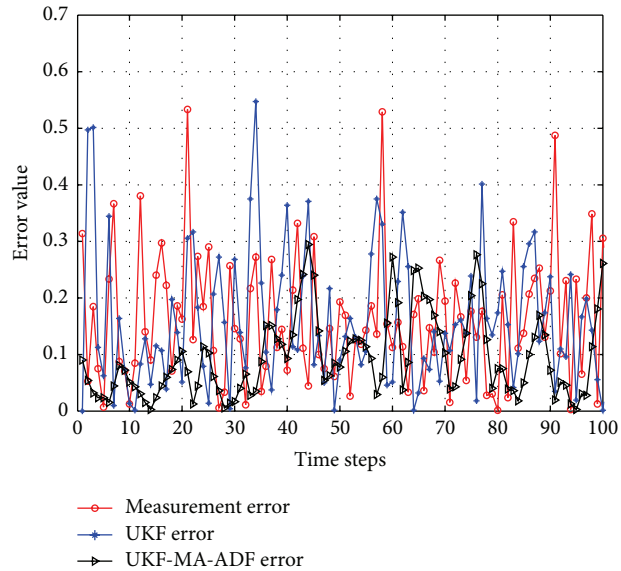

Figure 4: Contrast of filter processing error.

As can be seen from Figure 4, signals processed through UKF have larger errors, while those processed by the UKF- and wavelet analysis-based multisensor adaptive weighted data fusion algorithm proposed herein have the smallest errors, indicating that the proposed algorithm is effective in data filtering processing. Compared with other algorithms, our algorithm had higher accuracy and was closer to the actual measurement values.

In order to better illustrate the effect of these filter algorithms, mean absolute error (MAE), maximum relative error (Max RE), and root mean square error (RMSE) are adopted for evaluation; they are, respectively, defined as follows: $\text{MAE} = (1/n)\sum_{k=1}^{n} |x_k - x_k'|$, $\text{Max RE} = \max |x_k - x_k'|$, $\text{RMSE} = \sqrt{\sum_{k=1}^{n}(x_k - x_k')^2/n}$, where x_k is the actual value measured by the sensor and x_k' is the value filtered and processed by unscented Kalman filter (Method 1) and wavelet

Table 1: Comparison of several algorithms of error values.

Method	MAE	Max RE	RMSE
The measured value	0.168	0.697	0.186
UKF	0.135	0.531	0.168
UKF-MA-ADF	0.033	0.219	0.069

Table 2: Comparison of several algorithms of error values.

Method	MAE	Max RE	RMSE
The measured value	0.191	0.762	0.199
UKF	0.147	0.469	0.153
UKF-MA-ADF	0.045	0.201	0.103

analysis (Method 2); it is also a result of merged data utilizing adaptive weighted data fusion with three-way sensor data (Method 3); n is the number of samples. Comparison of algorithm error is shown in Table 1.

We can see from the simulation examples and the comparison of error indicators such as mean absolute error (MAE), maximum relative error (Max RE), and root mean square error (RMSE) that the UKF- and wavelet analysis-based multisensor adaptive weighted data fusion algorithm proposed herein have higher data filtering accuracy and are closer to the actual measurement values compared to the original measurement and UKF algorithm.

Assuming that the ideal sensor signals were a set of cosine signals $X(n)$, measurement signals were the cosine signals plus the random disturbance noise, and the measurement signals of sensors 1, 2, and 3 were $S_1 = X(n)+\text{rand}\,n(1,1024)*0.2$, $S_2 = X(n)+\text{rand}\,n(1,1024)*0.3$, and $S_3 = X(n)+\text{rand}\,n(1,1024)*0.4$, respectively, and signal filtering was performed on these sensor measurement signals in the same way. Taking the measurement signal S_1 as an example, the filtering results are shown in Figure 5. Figure 6 gives the comparison of errors after the filtering. Comparison of error values among various algorithms is shown in Table 2.

As can be seen from Figures 5 and 6, the proposed signal filtering method is also effective for cosine analog signals. Signals processed through UKF had larger errors, while those processed by the proposed UKF- and wavelet analysis-based adaptive weighted data fusion algorithm had the smallest errors. Our algorithm had higher measurement accuracy and was closer to the actual measurement values.

(2) Actual Measurement. The experiment was done under sunny, no wind, and low humidity conditions. The purpose of experiment was target detection and recognition of small moving vehicles using magnetoresistive sensors, where small and big vehicles were distinguished by magnetic flux. We used Honeywell HMC5883L magnetoresistive sensors to measure changes in the magnetic field when small vehicles passed through. Due to the directivity problem of magnetoresistive sensor, in this experiment, the $+Z$-axis direction of three magnetoresistive sensors was perpendicular to and facing the road surface, $+Y$-axis direction of the magnetoresistive

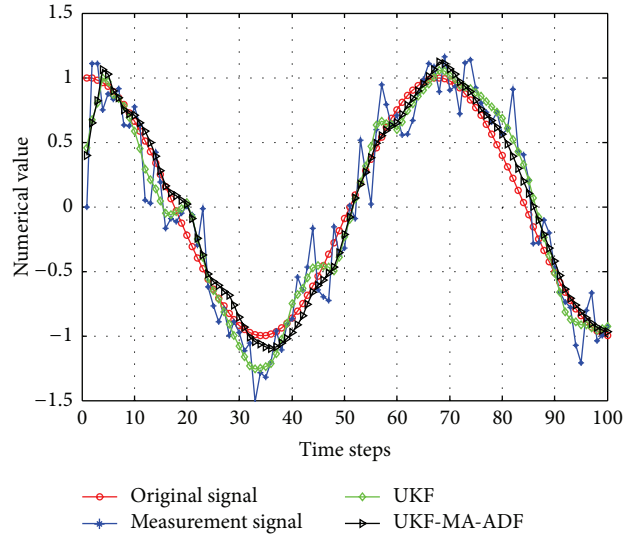

Figure 5: Simulation results of cosine signal filtering processing.

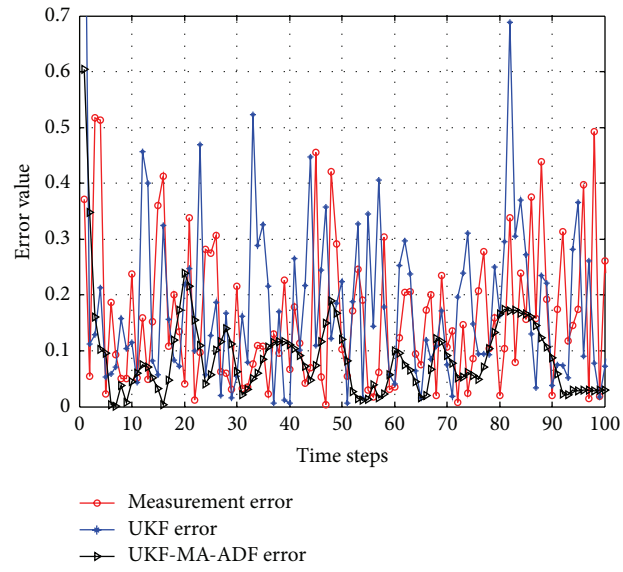

Figure 6: Contrast of filter processing error.

sensors was parallel with the road surface, while the $+X$-axis direction was perpendicular to the other two axes. To examine the measurement effect and resolution direction of magnetoresistive sensors, in this experiment, small vehicles were designed to travel at a 10 m/s constant speed, and three magnetoresistive sensors were placed separately on the vehicles' travel routes. To ensure the magnetic detection accuracy of magnetoresistive sensors, experiment was repeated multiple times by letting small vehicles travel back and forth at places 3 m away from the magnetoresistive sensors, and one set of data of three magnetoresistive sensors were selected among them for data processing. Data of three magnetoresistive sensors were named S_1, S_2, and S_3, respectively. To avoid significant data difference from affecting the accuracy of data processing, we normalized the data to interval

Table 3: Comparison of several algorithms of error values.

Method	MAE	Max RE	RMSE
The measured value	0.057	0.102	0.176
UKF	0.048	0.089	0.128
UKF-MA-ADF	0.031	0.058	0.084

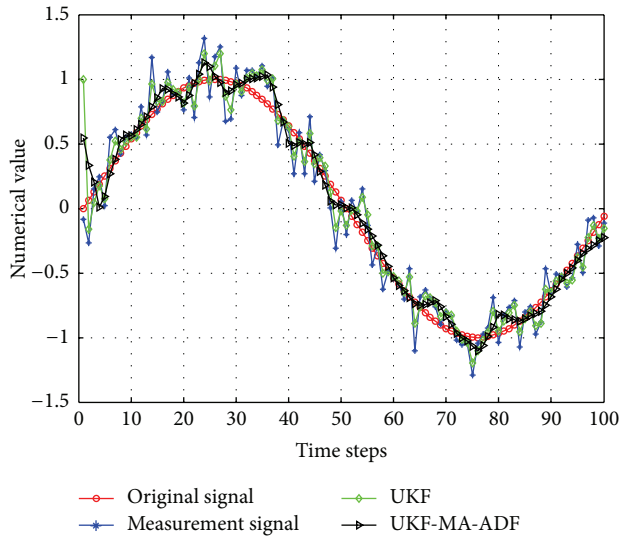

Figure 7: Simulation results of measured magnetic sensor signal filtering processing.

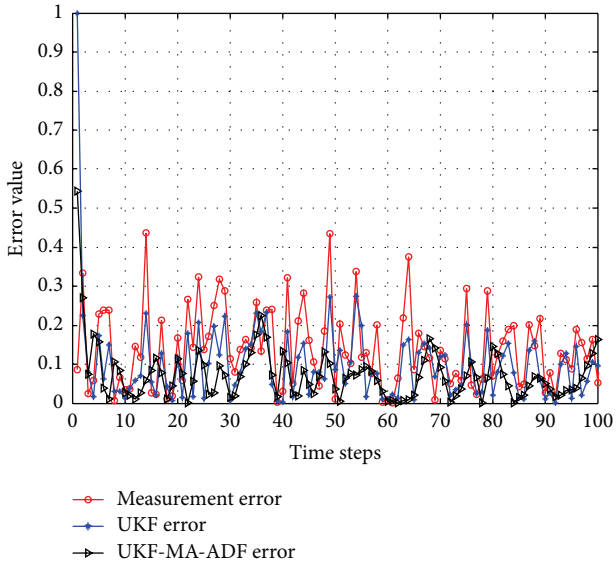

Figure 8: Contrast of filter processing error.

[0, 1]. In the same way as simulation, we performed UKF, multiscale wavelet decomposition, and reconstruction and adaptive data fusion filtering on these three sets of normalized measurement signals S_1, S_2, and S_3. Signals filtered through the above methods are shown in Figure 7. Figure 8 gives the comparison of errors after the filtering. Comparison of error values among various algorithms is shown in Table 3.

As can be seen from Figures 7 and 8 and Table 3, UKF, wavelet analysis, and adaptive fusion algorithm are effective in filtering the measurement signals, which can well retain the original measurement signals and allow more stable and smooth signals. Signals processed through UKF had larger errors, while those processed by the proposed UKF- and wavelet analysis-based adaptive weighted data fusion algorithm had the smallest errors. Our algorithm had higher measurement accuracy and was closer to the actual measurement values. In addition, comparison of error indicators showed that the UKF- and wavelet analysis-based multisensor adaptive weighted data fusion algorithm proposed herein had higher data filtering accuracy, smaller errors, and more accurate measurements compared to the original measurement and UKF algorithm.

7. Conclusion and Future Work

As one of the key intelligent measurement technologies, multisensor data fusion integrates the temporal and spatial complementary and redundant information of each sensor according to certain optimization criteria through reasonable control and use of multiple sensors and their observational data fully utilizing multiple sensor resources to produce a consistent interpretation and description of the observational environment. This paper proposes a new UKF-based multiscale adaptive fusion estimation algorithm by combining the multiscale signal analysis and UKF with the multisensor data fusion technology based on the given state model at a certain scale and the multisensor distributed dynamic system having different sampling rates at different scales. Global information-based fusion estimation values are obtained at the finest scale, and the effectiveness of the algorithm is verified by computer simulation, so as to ensure the reliability and accuracy of the sensor measurement system. This paper only gives examples in one-dimensional context. Further experimental verification combining practical application is needed in future for cases where the state vector is multidimensional.

Conflict of Interests

The authors declare that there is no conflict of interests regarding the publication of this paper.

Acknowledgments

The authors would like to thank the anonymous reviewers for helpful comments which helped them improve the technical quality of the paper. This study was supported by the National Natural Science Foundation of China (Grant no. U1504602), Postdoctoral Science Foundation of China (2015M572141), and the project of Foundation and Cutting-Edge Technologies in Henan Province of China (142300410339; 132300410479).

References

[1] M. Munz, M. Mählisch, and K. Dietmayer, "Generic centralized multi sensor data fusion based on probabilistic sensor and environment models for driver assistance systems," *IEEE Intelligent Transportation Systems Magazine*, vol. 2, no. 1, pp. 6–17, 2010.

[2] Z. Zhou, Y. Li, J. Liu, and G. Li, "Equality constrained robust measurement fusion for adaptive kalman-filter-based heterogeneous multi-sensor navigation," *IEEE Transactions on Aerospace and Electronic Systems*, vol. 49, no. 4, pp. 2146–2157, 2013.

[3] W. Liu, J. Wei, M. Liang, Y. Cao, and I. Hwang, "Multi-sensor fusion and fault detection using hybrid estimation for air traffic surveillance," *IEEE Transactions on Aerospace and Electronic Systems*, vol. 49, no. 4, pp. 2323–2339, 2013.

[4] S. L. Sun, X. Y. Li, and S. W. Yan, "Estimators for autoregressive moving average signals with multiple sensors of different missing measurement rates," *IET Signal Processing*, vol. 6, no. 3, pp. 178–185, 2012.

[5] M. Chen and M. L. Fowler, "Data compression for multi-parameter estimation for emitter location," *IEEE Transactions on Aerospace and Electronic Systems*, vol. 46, no. 1, pp. 308–322, 2010.

[6] H. Zhao and Z. Wang, "Motion measurement using inertial sensors, ultrasonic sensors, and magnetometers with extended kalman filter for data fusion," *IEEE Sensors Journal*, vol. 12, no. 5, pp. 943–953, 2012.

[7] Y.-S. Chiou and F. Tsai, "A reduced-complexity data-fusion algorithm using belief propagation for location tracking in heterogeneous observations," *IEEE Transactions on Cybernetics*, vol. 44, no. 6, pp. 922–935, 2014.

[8] G. Ligorio and A. M. Sabatini, "A novel Kalman filter for human motion tracking with an inertial-based dynamic inclinometer," *IEEE Transactions on Biomedical Engineering*, vol. 62, no. 8, pp. 2033–2043, 2015.

[9] A. Vaccarella, E. de Momi, A. Enquobahrie, and G. Ferrigno, "Unscented Kalman filter based sensor fusion for robust optical and electromagnetic tracking in surgical navigation," *IEEE Transactions on Instrumentation and Measurement*, vol. 62, no. 7, pp. 2067–2081, 2013.

[10] Z.-Q. Zhang, L.-Y. Ji, Z.-P. Huang, and J.-K. Wu, "Adaptive information fusion for human upper limb movement estimation," *IEEE Transactions on Systems, Man, and Cybernetics A:Systems and Humans*, vol. 42, no. 5, pp. 1100–1108, 2012.

[11] Y. Zheng, R. Niu, and P. K. Varshney, "Sequential bayesian estimation with censored data for multi-sensor systems," *IEEE Transactions on Signal Processing*, vol. 62, no. 10, pp. 2626–2641, 2014.

[12] M. Mosallaei and K. Salahshoor, "Comparison of centralized multi-sensor measurement and state fusion methods with an adaptive unscented kalman filter for process fault diagnosis," in *Proceedings of the 4th International Conference on Information and Automation for Sustainability (ICIAFS '08)*, pp. 519–524, Colombo, Sri Lanka, December 2008.

[13] F. Cappello, S. Ramasamy, R. Sabatini, and J. Liu, "Low-cost sensors based multi-sensor data fusion techniques for RPAS navigation and guidance," in *Proceedings of the International Conference on Unmanned Aircraft Systems (ICUAS '15)*, pp. 714–722, Denver, Colo, USA, June 2015.

[14] Y. Wang, Y. Jia, J. Du, and F. Yu, "Bearings-only multi-sensor multi-target tracking based on Rao-Blackwellized Monte Carlo data association," in *Proceedings of the 29th Chinese Control Conference (CCC '10)*, pp. 1126–1131, Beijing, China, July 2010.

[15] X. Wang, H. Hu, and X. Liu, "Multisensor data fusion techniques with ELM for pulverized-fuel flow concentration measurement in cofired power plant," *IEEE Transactions on Instrumentation and Measurement*, vol. 64, no. 10, pp. 2769–2780, 2015.

[16] R. K. Young, *Wavelet Theory and Its Applications*, Springer Science & Business Media, 2012.

[17] C. Cattani, "Fractional calculus and Shannon wavelet," *Mathematical Problems in Engineering*, vol. 2012, Article ID 502812, 26 pages, 2012.

[18] D. K. Ruch and P. J. Van Fleet, *Wavelet Theory: An Elementary Approach with Applications*, John Wiley & Sons, 2011.

[19] F. In and S. Kim, *An Introduction to Wavelet Theory in Finance: A Wavelet Multiscale Approach*, World Scientific, 2012.

[20] C. E. D'Attellis and E. M. Fernandez-Berdaguer, *Wavelet Theory and Harmonic Analysis in Applied Sciences*, Springer, 2012.

[21] L.-W. Fong, "Multi-sensor data fusion via federated adaptive filter," in *Proceedings of the IEEE International Symposium on Computer, Communication, Control and Automation (3CA '10)*, vol. 1, pp. 209–212, Tainan, Taiwan, May 2010.